Supplementary information

Closing the loop for Poly(butylene-adipate-co-terephthalate) recycling: Depolymerization, monomers separation and upcycling

Mohamad Ismail[1*], Adel Abouhmad[1,2], Niklas Warlin[1,3], Sang-Hyun Pyo[1], Oliver Englund Örn[1], Basel Al-Rudainy[4], Cecilia Tullberg[1], Baozhong Zhang[3], Rajni Hatti-Kaul[1*]

[1]Division of Biotechnology, Department of Chemistry, Centre for Chemistry and Chemical Engineering, Lund University, SE-221 00 Lund, Sweden

[2]Department of Microbiology and Immunology, Faculty of Pharmacy, Al-Azhar University, Assiut 71524, Egypt

[3]Centre of Analysis and Synthesis, Department of Chemistry, Lund University, P.O. Box 124, SE-22100 Lund, Sweden.

[4]Department of Chemical Engineering, Centre for Chemistry and Chemical Engineering, Lund University, SE-221 00 Lund, Sweden

* *Corresponding author*

Cloning and expression of Leaf-branch compost cutinase (LCC-WCCG)

The nucleotide sequence of LCC-WCCG [F243W/D238C/S283C/Y127G] after substitution of the N-terminal signal peptide with 6-His tag was codon optimized for expression in *E. coli* and ordered as a gBlock gene fragment from Integrated DNA Technologies (IDT, Leuven, Belgium). Cloning of His_6-LCC-WCCG gBlock was performed as reported earlier.[1] The gene was inserted between *Nco*I and *Xho*I restriction sites of the expression vector pET28a(+) followed by ligation with T4 DNA ligase and transformation of the ligation mixture into *E. coli* BL21(DE3). The cells were plated on LB agar plates supplemented with 50 μg mL^{-1} kanamycin and grown overnight at 37 °C. Plasmids extracted from the transformant colonies were sequenced (GATC Biotech AB, Solna, Sweden), and those with correct sequences were used for protein expression in *E. coli* BL21(DE3). Glycerol stock of (His_6-LCC-WCCG-pET28a(+))-*E. coli* BL21(DE3) was prepared by growing the cells overnight at 37 ˚C, 200 rpm in LB medium supplemented with 50 μg mL^{-1} kanamycin, and then mixing with 50% glycerol, prior to distributing in 1 mL aliquots for storage at -80 °C.

For enzyme production, glycerol stock of the recombinant *E. coli* BL21(DE3) cells harbouring (His_6-LCC-WCCG-pET28a(+)) plasmid were first inoculated into 25 mL of LB medium supplemented with 50 μg mL^{-1} kanamycin in 250 mL sterile flask and grown overnight at 37 ˚C, 200 rpm. The preculture was used to inoculate 300 mL of auto-induction medium (1% tryptone, 0.5%, yeast extract, 25 mM Na_2HPO_4, 25 mM KH_2PO_4, 25 mM $(NH_4)_2SO_4$, 2 mM $MgSO_4$, 0.05% glucose and 0.2% α-lactose) supplemented with 100 μg mL^{-1} kanamycin, in 1 L Erlenmeyer flask to an OD_{600nm} of 0.1. The culture was incubated at 37 °C, 200 rpm for 5 h, and then at 16 °C for 24 h prior to harvesting the cells by centrifugation at 6000 rpm, 4 °C for 20 min (Sorvall Lynx 4000 centrifuge, Thermo Scientific).

Purification of His_6-LCC-WCCG

Purification of His tagged LCC-WCCG was done by immobilized metal ion chromatography. The cell pellet obtained above was suspended in the binding buffer (100 mM Tris-HCl, 20 mM imidazole, 0.5 M NaCl, pH 8) at a concentration of 1 gm cells (wet weight) in 10 mL binding buffer and sonicated on ice (5 X, 60 s, cycle 0.5) using UP400S sonicator (Dr. Hielscher GmbH, Stahnsdorf, Teltow, Germany). The cell debris was removed by centrifugation at 14,000 rpm, 30 min, 4 °C (Sorvall LYNX 4000). The clarified cell lysate was filtered through a 0.2 μm filter and loaded on 5 mL HisTrap FF™ Nickel column (GE Healthcare Bio-Sciences AB, Uppsala, Sweden) pre-equilibrated with the binding buffer and connected to ÄKTA Start

chromatography system controlled by UNICORN software for fast protein liquid chromatography (FLPC, GE Healthcare) at a flow rate of 5 mL min^{-1}. Unbound proteins were removed by washing with the same buffer, and finally, the bound proteins were eluted with the elution buffer (100 mM Tris-HCl, 0.5 M NaCl, 0.5 M imidazole, pH 8). The purified protein was desalted on a 5 mL HiTrap desalting column (Sephadex G-25 Superfine resin, GE Healthcare) equilibrated with storage buffer (100 mM Tris-HCl, 500 mM NaCl, pH 8), analyzed by SDS-PAGE, and quantified with NanoDrop ND-1000 spectrophotometer (Thermo Scientific) and bicinchoninic acid (BCA) assay.

Analyses

HPLC and LC-MS analysis of PBAT monomers and BDO oxidation products

The monomers released from the hydrolysis of PBAT (AA, BDO), and the oxidation reaction products (succinic acid, and 4-hydroxybutanoic acid) were quantified using HPLC (JASCO, Tokyo, Japan) equipped with refractive index detector (ERC, Kawaguchi, Japan), a JASCO intelligent autosampler and a chromatographic oven (Shimadzu, Tokyo, Japan). Separation of AA and BDO was done on an Aminex HPX-87H column (100 x 7.8 mm) connected to a guard column (Biorad, Richmond, CA, USA), maintained at 65 °C and using 0.05 mM H_2SO_4 as mobile phase at flow rate of 0.6 mL min^{-1}. SA and 4-HB were separated on Aminex HPX-87H column (300 x 7.8 mm) at 65 °C using 5 mM H_2SO_4 as mobile phase. TPA was analysed on a C18 column (Kromasil, Sweden) connected to guard column (C18 Kromasil, Sweden) at 40 °C using 20 % acetonitrile with 0.02 % formic acid as mobile phase at 0.6 mL min^{-1} and JASCO UV detector at 215 nm. Samples were prepared by diluting in DMSO for TPA, AA, and BDO analysis. The detection limits for TPA, AA, and BDO are 0.5 µg ml^{-1}, 0.05 mg ml^{-1}, and 0.05 mg ml^{-1}, respectively.

HPLC-MS was employed for the analysis of initial oxidation reactions of BDO; Ultimate 3000 HPLC, equipped with a VelosPro linear iontrap MS (Thermo Fisher Scientific). Ascentis-Express HILIC (15 cm x 2.1 mm, 2.7 µm) column was used for separation of the compounds under investigation using A) 100 mM ammonium acetate and B) 100 % acetonitrile with a gradient method. The gradient used was 0-4 min 95% B to 50% B, 4-4.5 min 50 % B, 4.5-5 min 50 % to 95 % B, 5-6 min 95% B, 6-6.5 min 95% to 50 % B, 6.5-7 min 50% B, 7-7.5 min 50% to 95 % B and 7.5-11 min 95 % B.

NMR and other analyses for polymer characterization

^{1}H and ^{13}C NMR measurements were performed on a Bruker DR X400 spectrometer at 400.13 MHz and 100.61 MHz, respectively. Chemical shifts were reported as δ values (ppm). Size exclusion chromatography (SEC) measurements for the polyesters were carried out using Malvern Viscotek TDAmax instrument with two T6000M general mixed organic columns (8 × 300 mm) equipped with OmniSEC triple detectors (refractive index, viscosity, and light scattering) and chloroform as eluent at 35 °C at a flow rate of 1 mL min^{-1}. Calibration was performed with a narrow polystyrene standard (M_p = 9 630, Đ = 1.04). TGA measurements were carried out on a TA instrument mode TGA Q500. The samples were heated from 50–600 °C with a heating rate of 10 °C min^{-1}. DSC measurements were performed on DSC Q2000 analyzer from TA instruments. Data was recorded from -60 – 250 °C, and T_g was determined from the second heating cycle.

Scanning Electron Microscopy of PBAT films

PBAT films (6-9 mg, 0.5 × 1.0 cm each), treated with 0.125 µM of the purified LCC-WCCG in 100 mM potassium phosphate buffer pH 8 at 50 °C, 600 rpm for 24 and 48 hours, were examined by scanning electron microscopy. The film incubated under the same conditions in the absence of the enzyme served as control. The films were washed with Milli-Q water and dried by lyophilization. The dried films were critical-point dried (BAL-TEC CPD 030, Bal-Tec AG, Balzers, Liechtenstein), glued onto metal sockets, and sputter-coated with gold/palladium at 1.2 kV, 15 mA, 0.02 mbar (Polaron SC7640 sputter coater, Quorum Technologies Ltd, Kent, UK). The films were examined with a scanning electron microscope (SEM; JEOL JSM-5600LV, Jeol Ltd, Tokyo, Japan) at 7 kV, the areas of interest were photographed and recorded. Control (untreated PBAT) films were treated and examined under the same conditions for comparison.

Fourier-transform infrared spectroscopy (FTIR)

Ten microliter samples from the polymerization reaction between AA and HDMA were placed on the pedestal of a Nicolet™ iS™ 5 FTIR Spectrometer (Thermo Fisher Scientific, Waltham, MA, USA), and after the solvent evaporated the percent transmission was collected in the ZeSe window.

Equation S1: Conventional Michaelis-Menten kinetics model

$$v = \frac{{}^{Conv}V_{max} S_0}{{}^{Conv}K_m + S_0}$$

$$ {}^{Conv}V_{max} = K_{cat} E_0$$

${}^{Conv}V_{max}$, refers to the maximum reaction velocity, S_0 is concentration of the substrate (substrate load), ${}^{Conv}K_m$ is Michaelis constant of the conventional kinetic model.

${}^{Conv}V_{max}$, can be calculated from K_{cat} turnover number and E_0 enzyme concentration in the reaction.

Equation S2: Inverse Michaelis-Menten kinetics model

$$v = \frac{{}^{Inv}V_{max} E_0}{{}^{Inv}K_m + E_0}$$

$${}^{Inv}V_{max} = K_{cat} \Gamma E_0$$

${}^{Inv}V_{max}$ is the maximum reaction velocity calculated from inverse kinetic model, E_0 is enzyme concentration used in the reactions, ${}^{Inv}K_M$ is Michaelis constant of the inverse model.

${}^{Inv}V_{max}$ can be calculated using *Kcat*, Γ reactive site density, and E_0 enzyme concentration.

Equation S3: Reactive site density equation

$$\Gamma = \frac{{}^{Inv}V_{max} / S_0}{{}^{Conv}V_{max} / E_0}$$

Γ Reactive site density can be calculated from both conventional and inverse kinetic models using equation S3

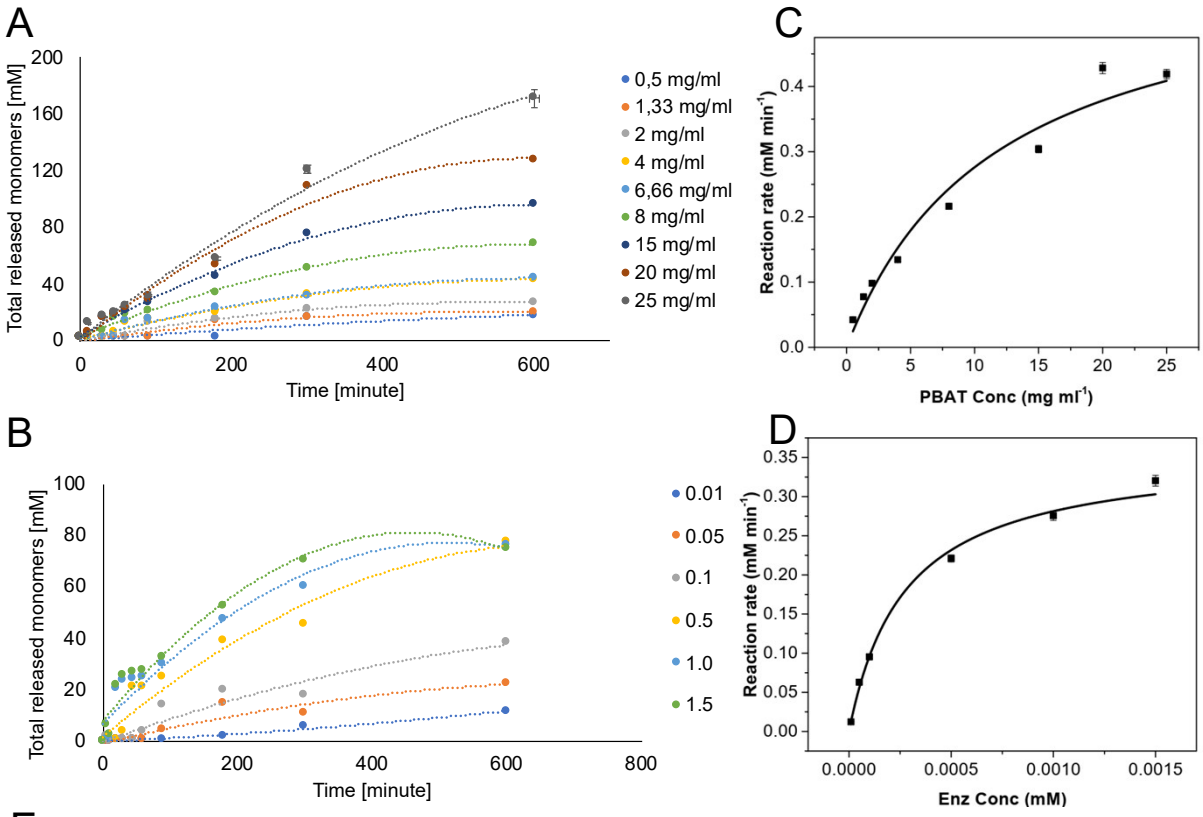

E

Enzyme	Specific activity [mg_{total} h^{-1} mg_{enz}^{-1}]	Conventional Kinetics				Inverse kinetics					
		V_{max} [mM min^{-1}]	K_m [mg ml^{-1}]	K_{cat} [min^{-1}]	K_{cat}/K_m [ml mg^{-1} min^{-1}]	V_{max} [mM min^{-1}]	K_m [mM^{-1}]	K_{cat} [min^{-1}]	V_{max}/S_0 [mmol g^{-1} min^{-1}]	K_{cat}/K_m [mM^{-1} min^{-1}]	Γ [mmol g^{-1}]
LCC-WCCG	65.77 ± 0.0	0.6 ± 0.09	11.7 ± 3.4	601 ± 93	51	0.35 ± 0.019	2.7x 10^{-4} ± 0.0	601 ± 20.7	3.5 x10^{-2} ± 0.0	2.2 x10^{6} ± 0.0	5.9x 10^{-5} ± 0.0

Figure S1. Kinetics measured for LCC-WCCG against PBAT. **(A, B)** Initial reaction rate curves showing total concentration of the released monomers (millimolar per minute). (**A**) Conventional kinetics model with variable substrate concentration (0.5-25 mg mL^{-1}) and fixed enzyme concentration, and (**B**) Inverse kinetics model using variable enzyme concentrations (0.01-1.5 µM) and fixed substrate concentration (10 mg mL^{-1}). Symbols are experimental data with a standard deviation of triplicates. **(C, D)** Michaelis-Menten (MM) plots for PBAT hydrolysis by LCC-WCCG from **(C)** conventional MM kinetics model, the curve shows the reaction rate as a function of PBAT concentration, and **(D)** inverse MM kinetic model, where the reaction rate is a function of the enzyme concentration. The plots were generated using the data from curves A and B. Error bars represent the standard deviation of reactions performed in triplicates. **(E)** Kinetic parameters calculated for LCC-WCCG catalysed hydrolysis of the PBAT polymer. The deviation error is generated from fitting triplicate measurements.

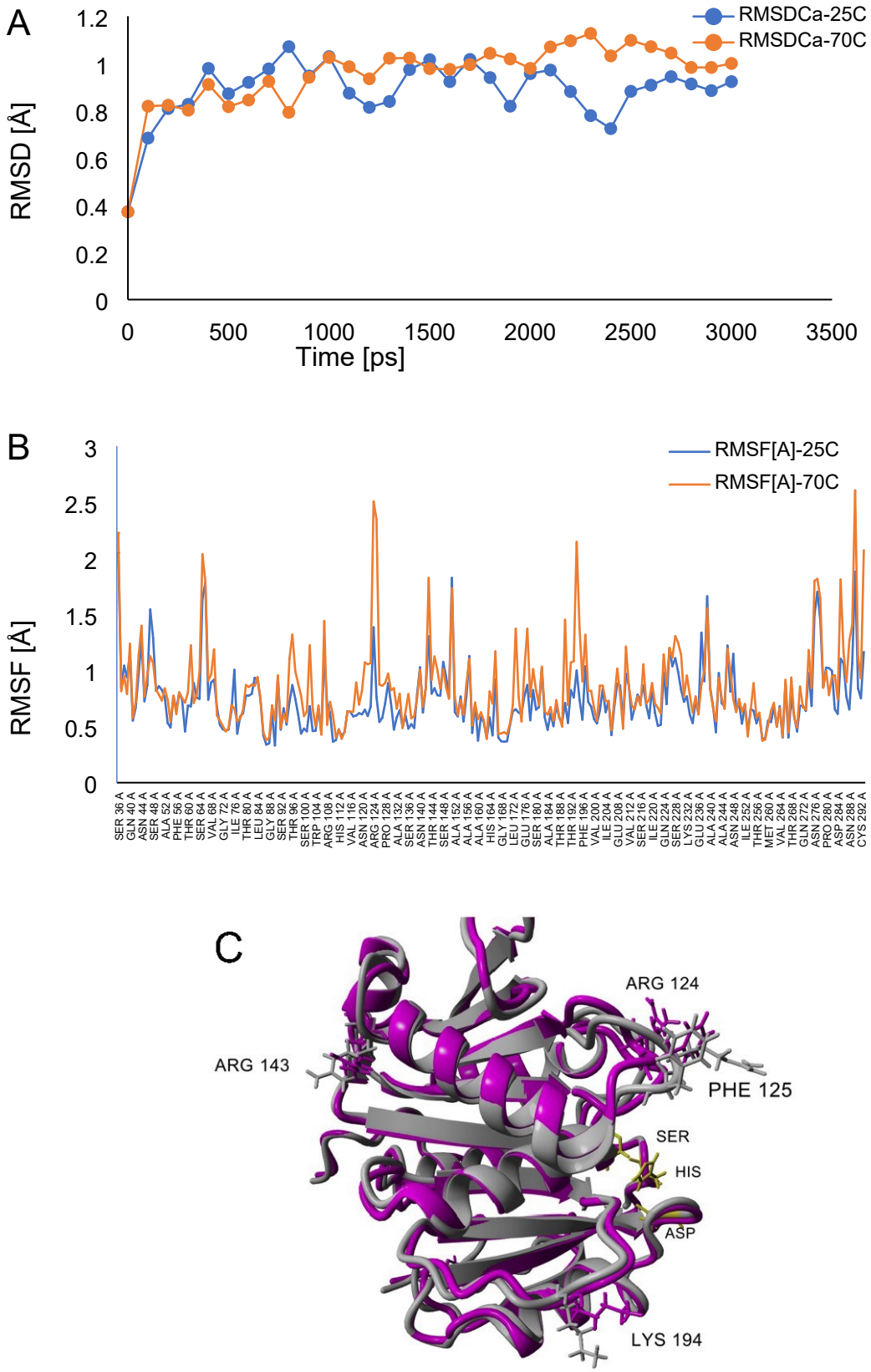

Figure S2. Overall change in the carbon backbone of the LCC-WCCG structure after 3 ns of MD simulation: **(A)** Root mean square deviation (RMSD) of backbone of LCC-WCCG structure at different temperatures, **(B)** Fluctuation of each residue of the LCC-WCCG structure at different temperature points. 0.4, 1, and 2.5 ns were selected for running the docking experiment. **(C)** Superimposed structures

after MD-simulation at 25 °C (magenta) and 70 °C (grey) indicating the most fluctuated residues at 70 °C. Simulation was done using YASARA structure, AMBER15IPQ was used as forcefield.

PBAT C1:
[O]C(C1=CC=C(C(OCCCCOC(CCCCC(OCCCCOC(C2=CC=C(C(OCCCCOC(CCCCC(OCCCCO)=O)=O)=O)C=C2)=O)=O)=O)=O)C=C1)=O

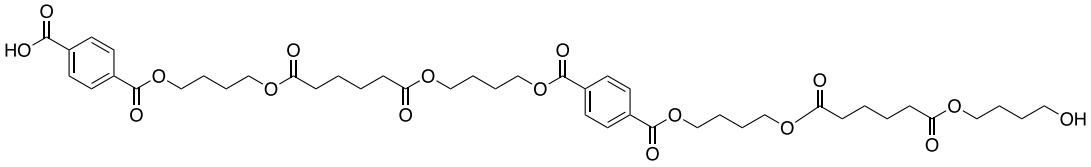

PBAT C2:
[O]C(C1=CC=C(C(OCCCCOC(CCCCC(OCCCCOC(CCCCC(OCCCCOC(C2=CC=C(C(OCCCCO)=O)C=C2)=O)=O)=O)=O)=O)=O)C=C1)=O

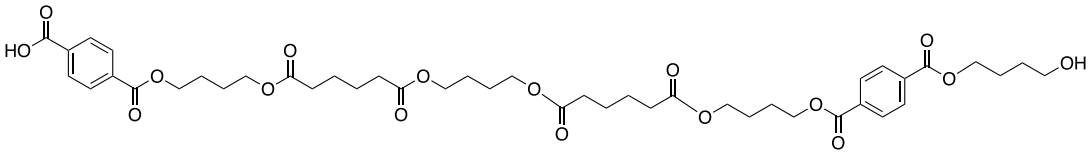

PET:
O=C(OCCO)C1=CC=C(C(OCCOC(C2=CC=C(C(OCCOC(C3=CC=C(C(OCCOC(C4=CC=C(C(OCCO)=O)C=C4)=O)=O)C=C3)=O)=O)C=C2)=O)=O)C=C1

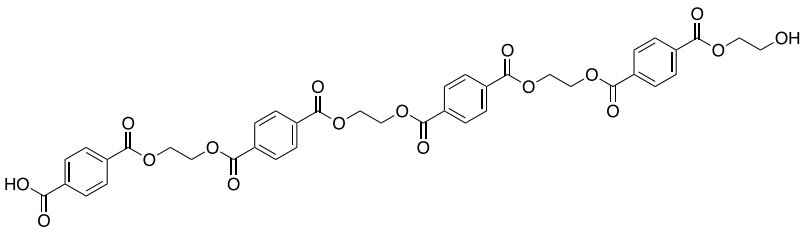

Figure S3. Different oligomers used in the docking studies including smiles and structures. Structures were drawn using ChemDraw 20.1, and 3D structures of the ligands were created using YASARA structure.

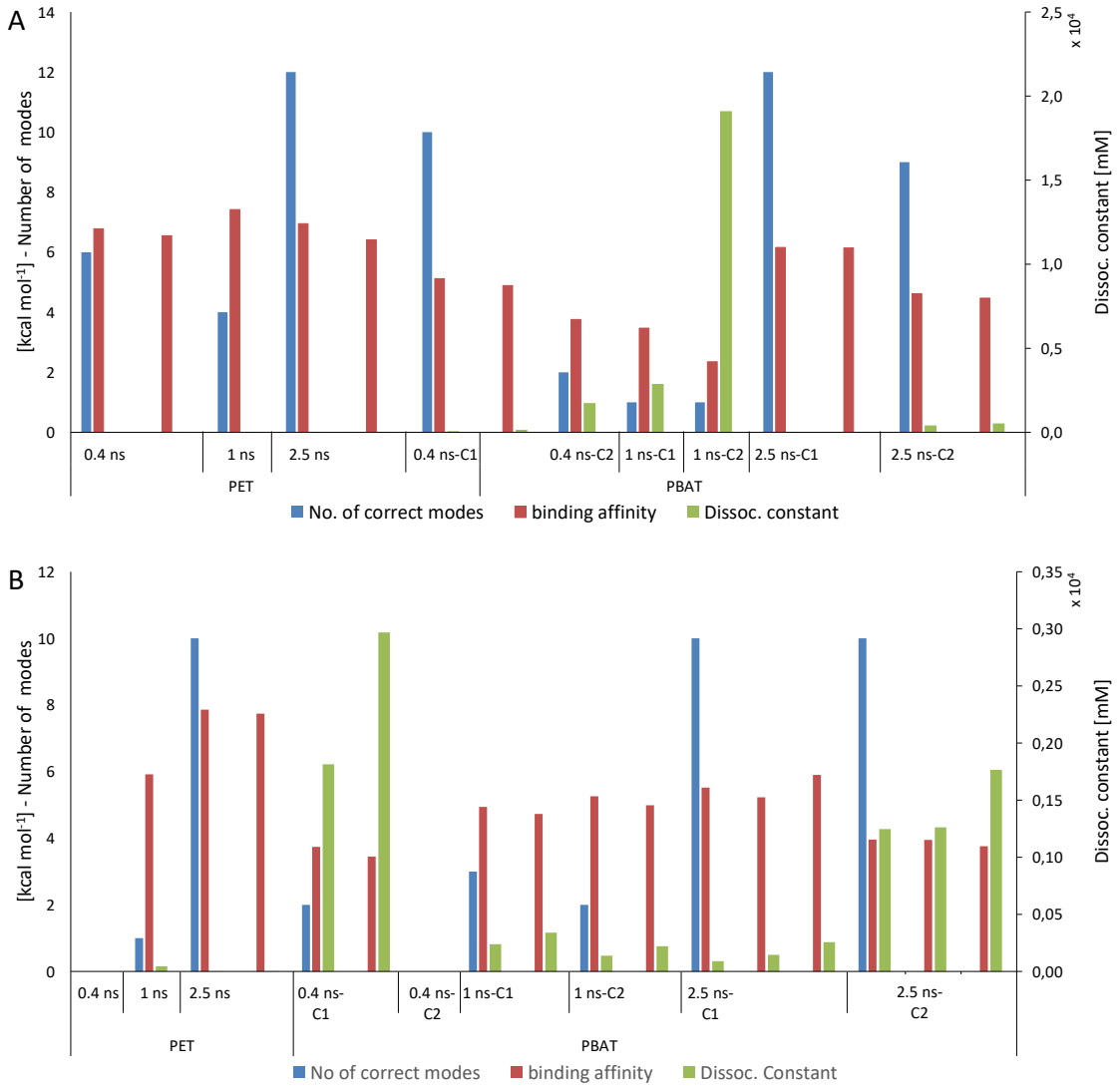

Figure S4. Docking results of PET and PBAT (different forms, PBAT-C1 and C2) (Figure S2) against LCC-WCCG as a receptor. **(A)** LCC-WCCG snapshots used for the docking study from MD-simulation at 25 °C, **(B)** LCC-WCCG snapshots from MD-simulation at 70 °C. More than one pose of the ligands is displayed based on their binding affinities. Docking was done using Vina with 25 runs and cluster RMSD of 5 Å. From the docking results 2.5 ns snapshot was found to be more suitable for further studies.

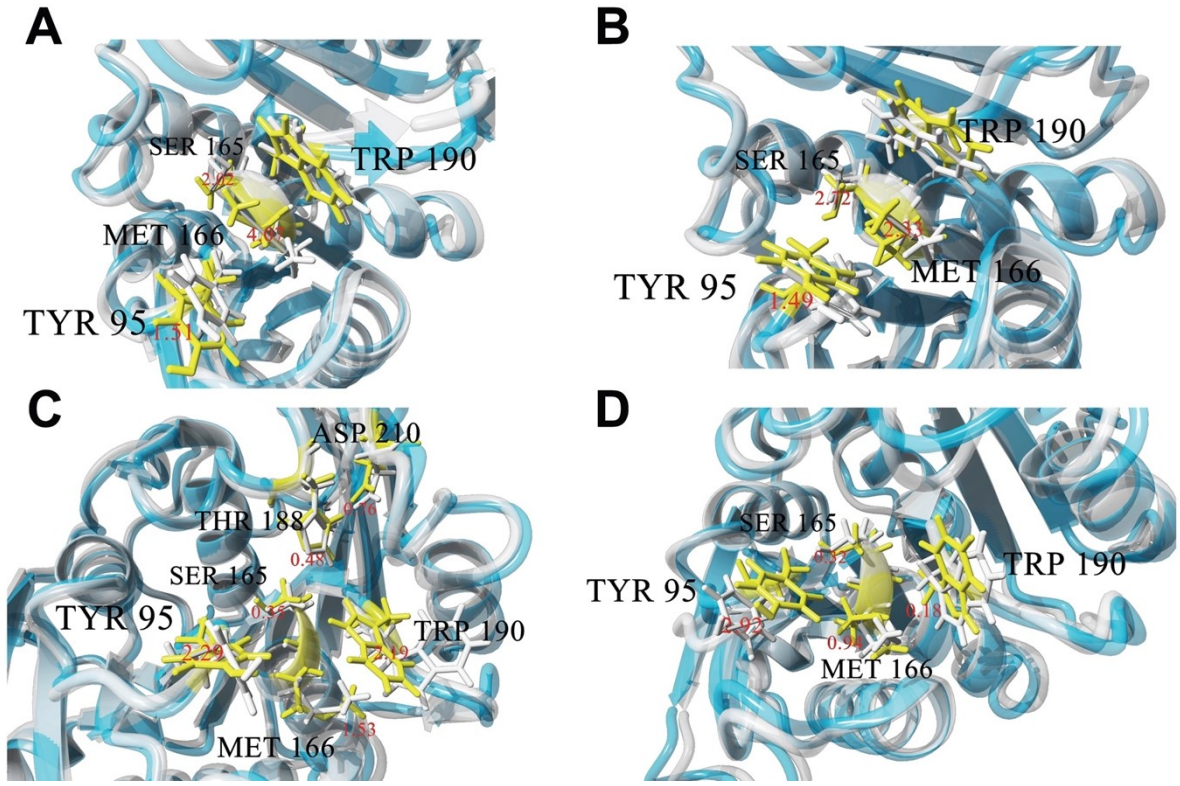

Figure S5. Deviation of the key residues (yellow after running MD-simulation for 2 ns for the best docking poses of PBAT C1 and C2. **(A)** PBAT-C1 MD-simulation at 25 °C, **(B)** PBAT-C1 MD-simulation at 70 °C **(C)** PBAT-C2 MD-simulation at 25 °C, **(D)** PBAT-C2 MD-simulation at 70 °C. Deviation distance is in red.

Table S1. Deviation of key residues, including catalytic triad after 2 ns of MD-simulation at 25 and 70 °C.

Structure	Temp (°C)	Residues	RMSD (Å)	Distance (Å)
PBAT-C2	25	TYR 95	2.0	1.49
		SER 165	1.73	2.72
		MET 166	2.27	2.33
		THR 188	1.15	1.10
		TRP 190	0.9	0.87
		ASP210	1.07	1.01
PBAT-C2	70	TYR 95	2.66	2.92
		SER 165	0.72	0.32
		MET 166	1.76	0.94
		THR 188	1.24	0.88
		TRP 190	1.28	0.18
		ASP 210	0.90	0.81
PBAT-C1	25	TYR 95	1.37	1.51
		SER 165	1.19	2.02
		MET 166	2.72	4.07
		THR188	1.18	0.76
		TRP 190	0.75	0.41
		ASP210	0.84	0.82

PBAT-C1	70	TYR 95	1.99	2.29
		SER 165	0.46	0.35
		MET 166	1.34	1.53
		THR188	1.20	0.48
		TRP 190	3.98	2.19
		ASP210	1.01	0.76
PET	25	TYR 95	4.95	6.59
		SER 165	0.64	0.94
		MET 166	2.87	4.16
		THR188	1.13	
		TRP 190	0.98	1.05
		ASP210	0.71	
PET	70	TYR 95	3.65	4.61
		SER 165	0.51	0.24
		MET 166	2.38	2.86
		THR 188	0.91	0.71
		TRP 190	1.31	1.14
		ASP 210	0.91	0.41

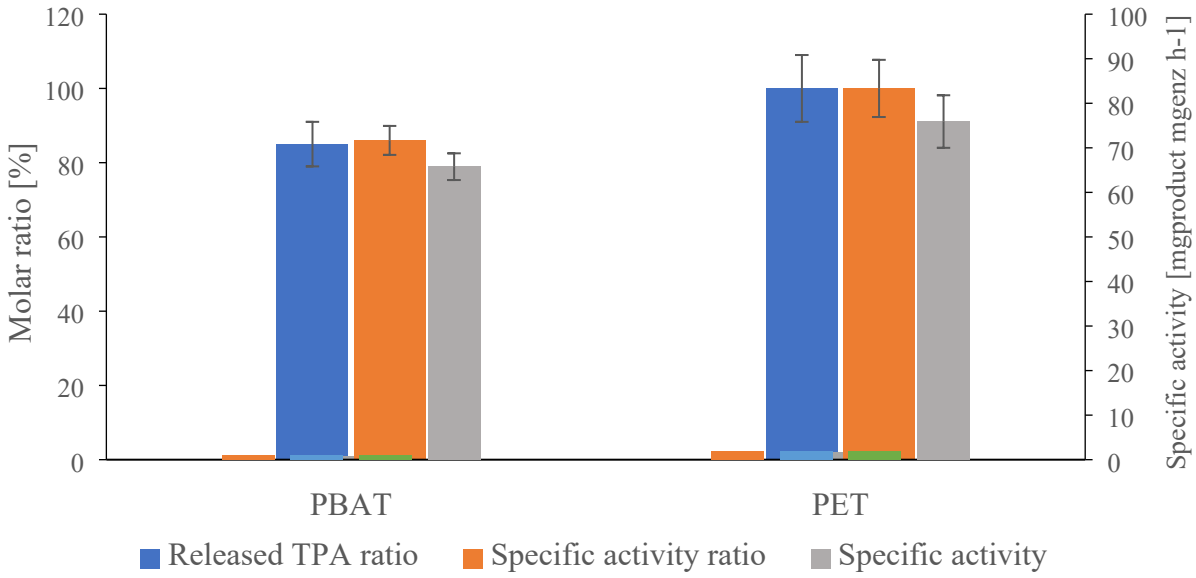

Figure S6. Activity of LCC-WCCG against PET and PBAT, based on ratio of released TPA (this study) and its specific activity against PBAT (this study) and PET (Tournier *et al*. 2020).[1] Reactions were done in duplicates using PET or PBAT particles (5 mg mL^{-1}) with 0.5 µM of LCC-WCCG in 100 mM Phosphate buffer pH 8. Samples were taken after 24 hours from the reaction. For the specific activity measurements, the reactions were done following the conditions described in table S3.

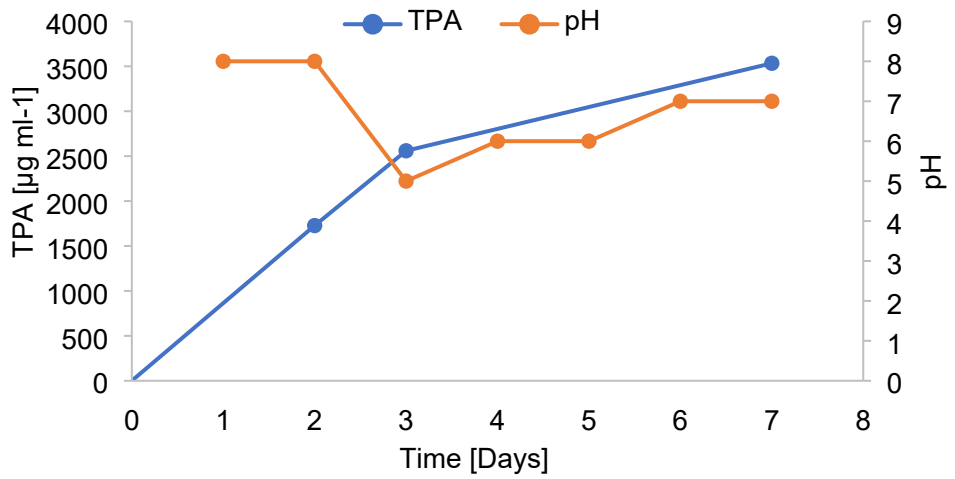

Figure S7. PBAT (12.5 g L^{-1}) depolymerisation using 1.65 µM, 2.5 mg LCC-WCCG in 50 mL reaction volume at 70 °C. Reaction was run in a shaking flask with a sealed opening to reduce evaporation. Samples were taken for analysis of the released TPA, pH was adjusted by adding 1 M NaOH while sampling. The polymer weight loss achieved within 7 days was 97.5 %.

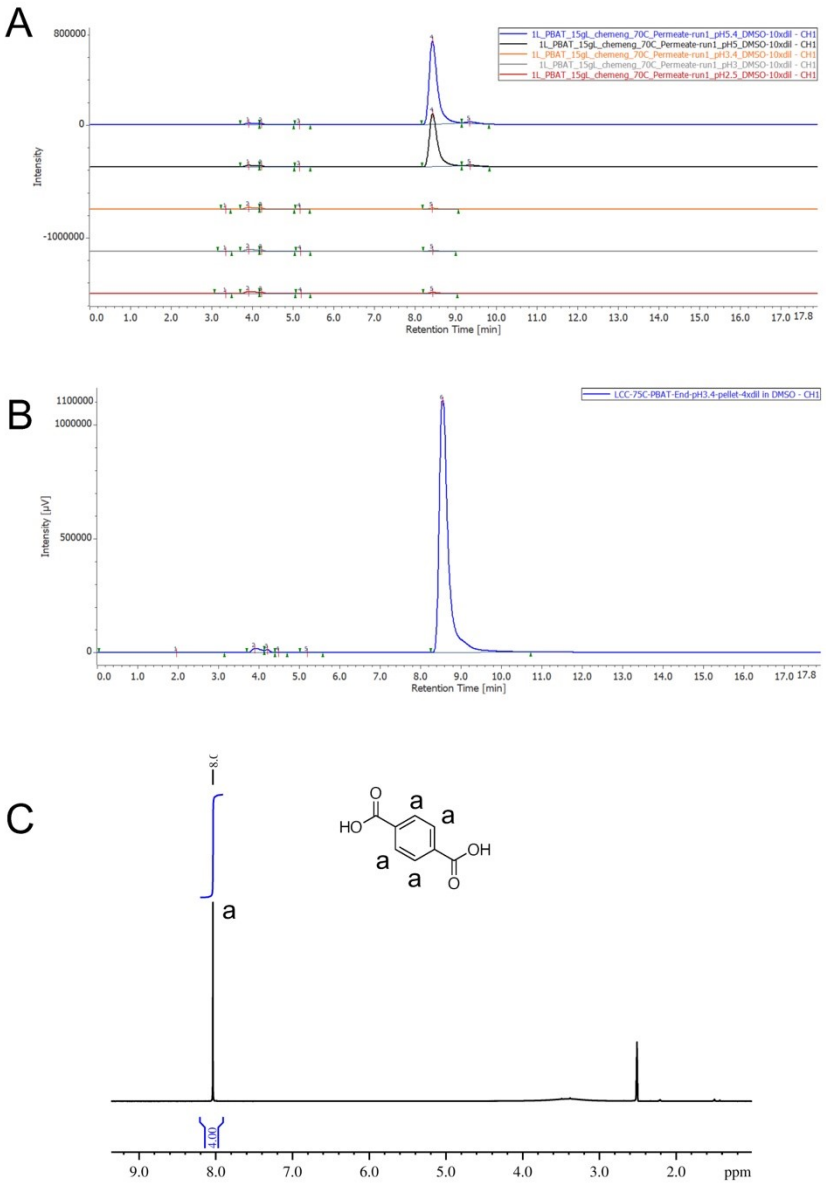

Figure S8. Terephthalic acid separation form PBAT hydrolysate, obtained by treatment of 15 g L^{-1} PBAT film in 1 Liter volume by LCC-WCCG, **(A)** gradual decrease in TPA concentration in the solution during stepwise acidification of the solution. **(B)** HPLC chromatogram of TPA purified from the reaction mixture at pH 2.5. **(C)** ^{1}H-NMR spectrum of the purified TPA in DMSO-d_6. The spectrum indicates nearly 5 % impurities from AA and BDO.

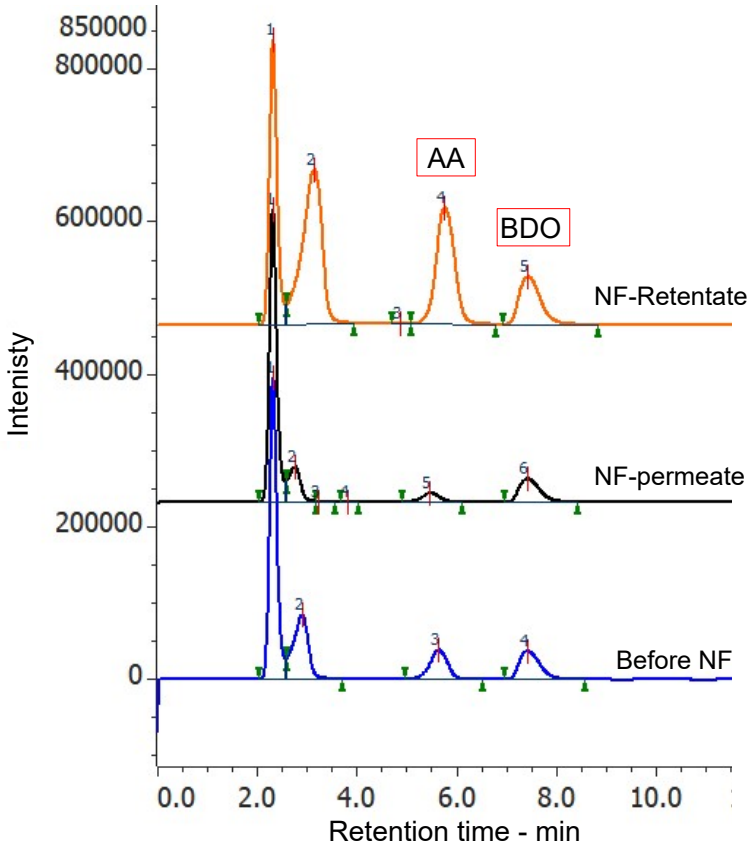

Figure S9. HPLC chromatograms showing adipic acid and 1,4-butanediol in the PBAT hydrolysate samples (after TPA separation) subjected to nanofiltration (before NF), and in retentate and permeate fractions obtained after nanofiltration. Peaks 1 and 2 are the injection and H_2SO_4 peaks from sample preparation.

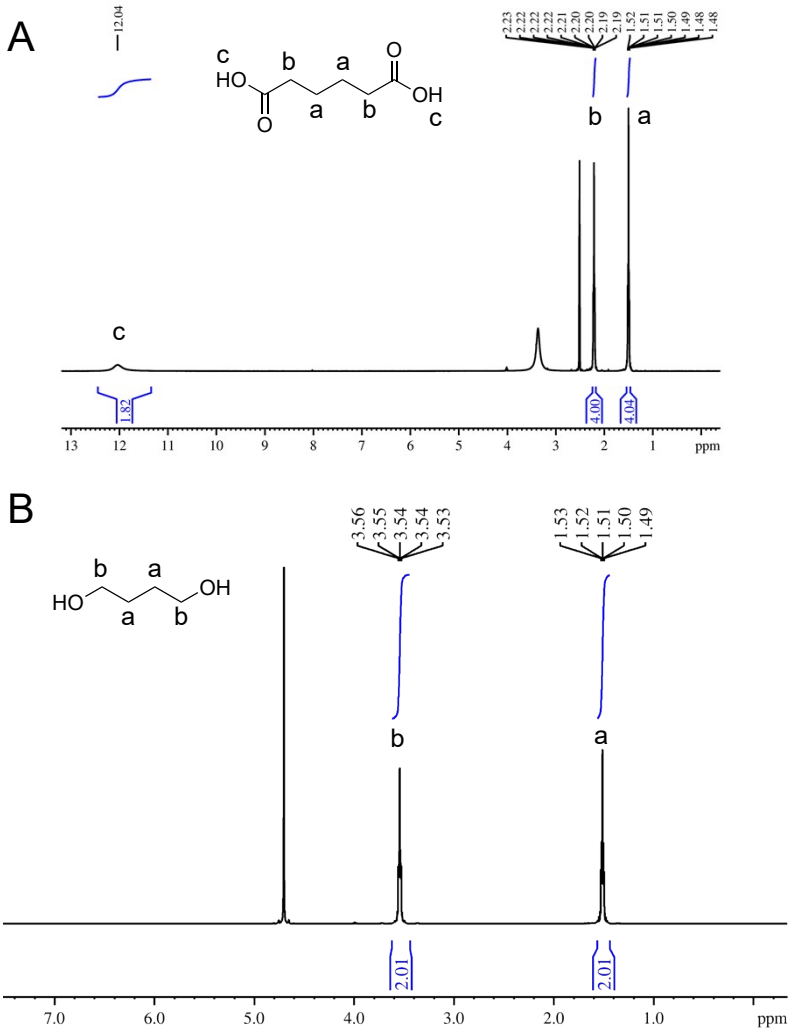

Figure S10. ^{1}H-NMR spectra of **(A)** AA in DMSO-d_6, purified from NF-retentate after separation from BDO by concentration and crystallization, and **(B)** BDO in D_2O, purified from NF-permeate after separation from AA.

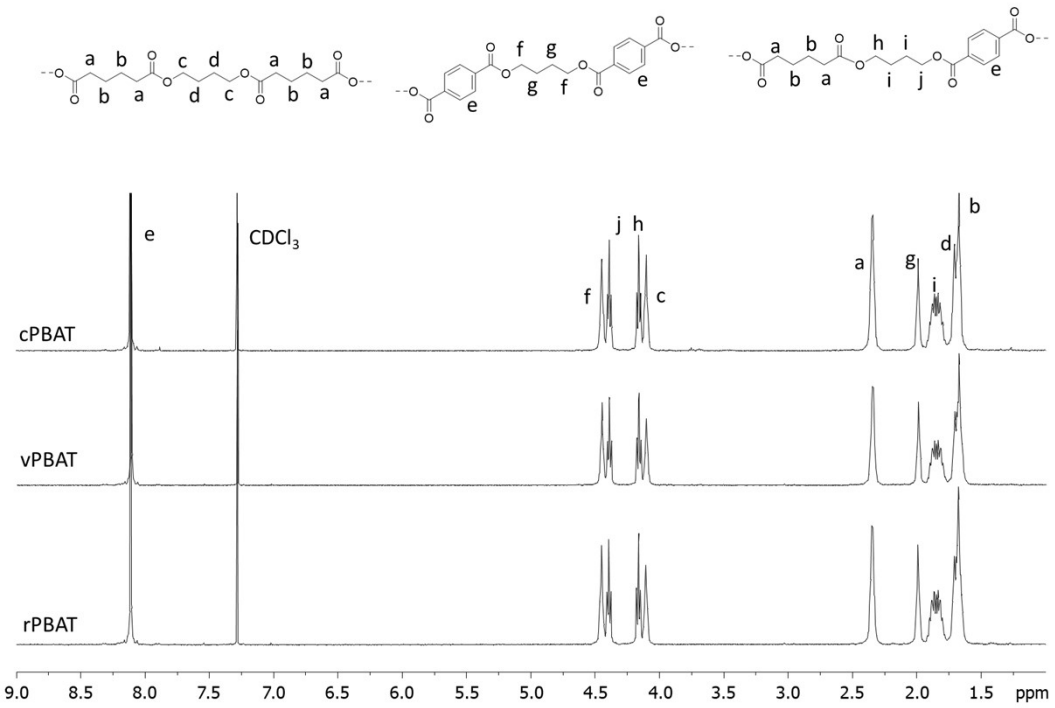

Figure S11. ^{1}H NMR spectra in $CDCl_3$ of the synthesized PBAT using commercial monomers (vPBAT) and recycled monomers (rPBAT), respectively. The ^{1}H NMR spectrum of a commercially available PBAT (cPBAT) was shown as well.

Sequence distribution analysis of PBAT

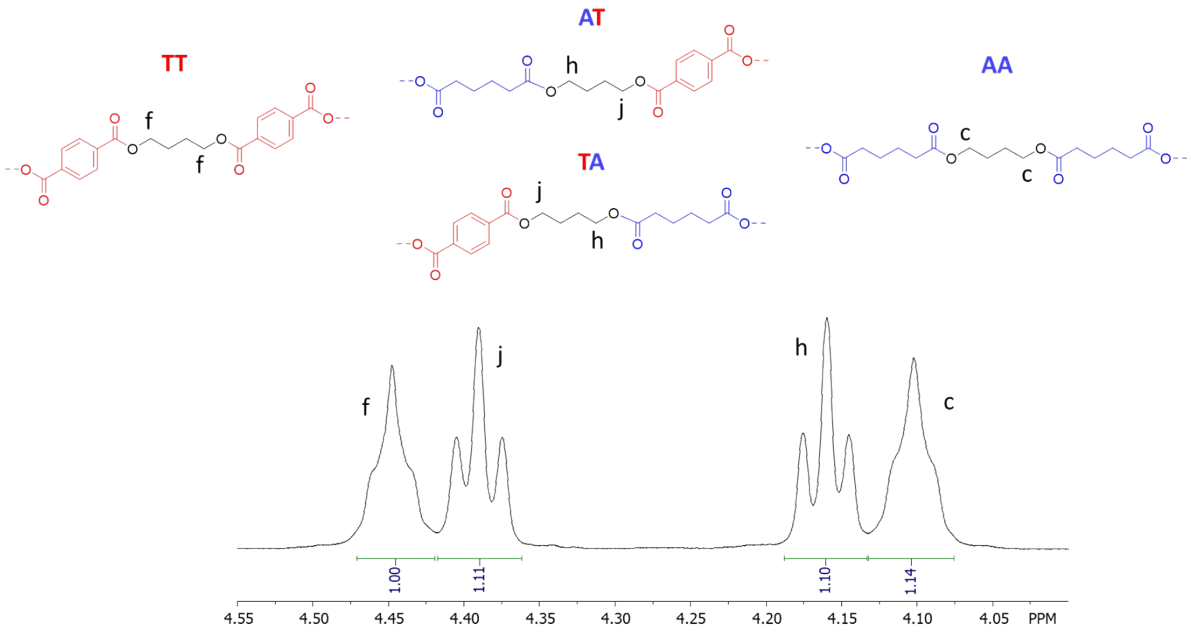

Figure S12. Zoomed-in figure of the ^{1}H NMR spectrum of cPBAT in $CDCl_3$ for sequence distribution calculations.

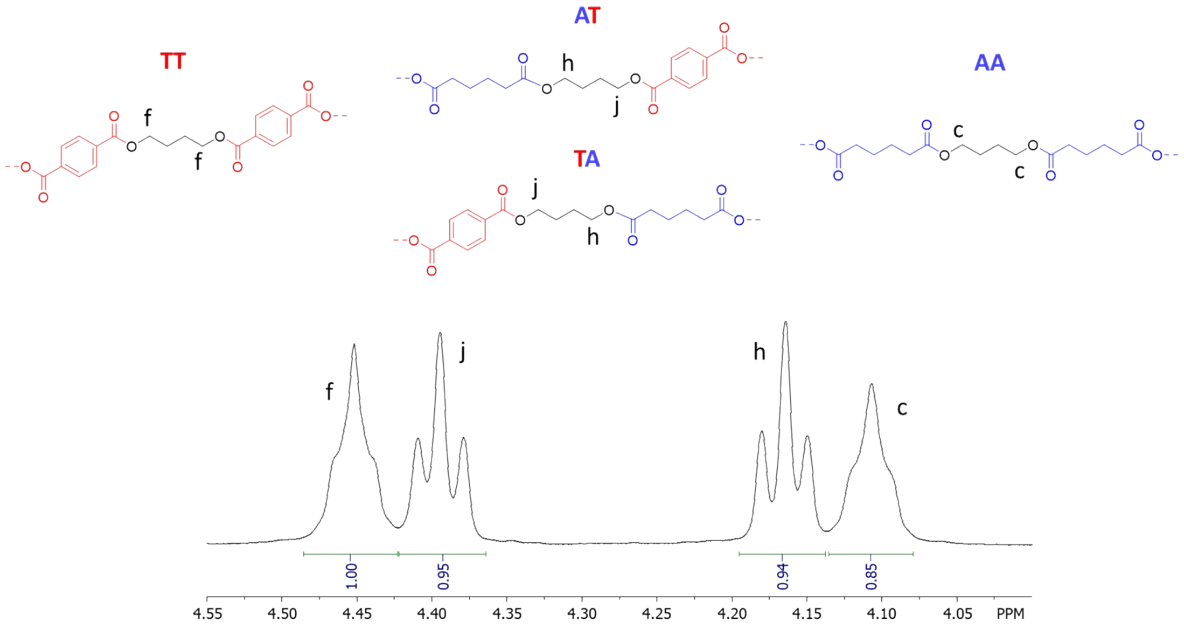

Figure S13. Zoomed-in figure of the ^{1}H-NMR spectrum of rPBAT in $CDCl_3$ for sequence distribution calculations.

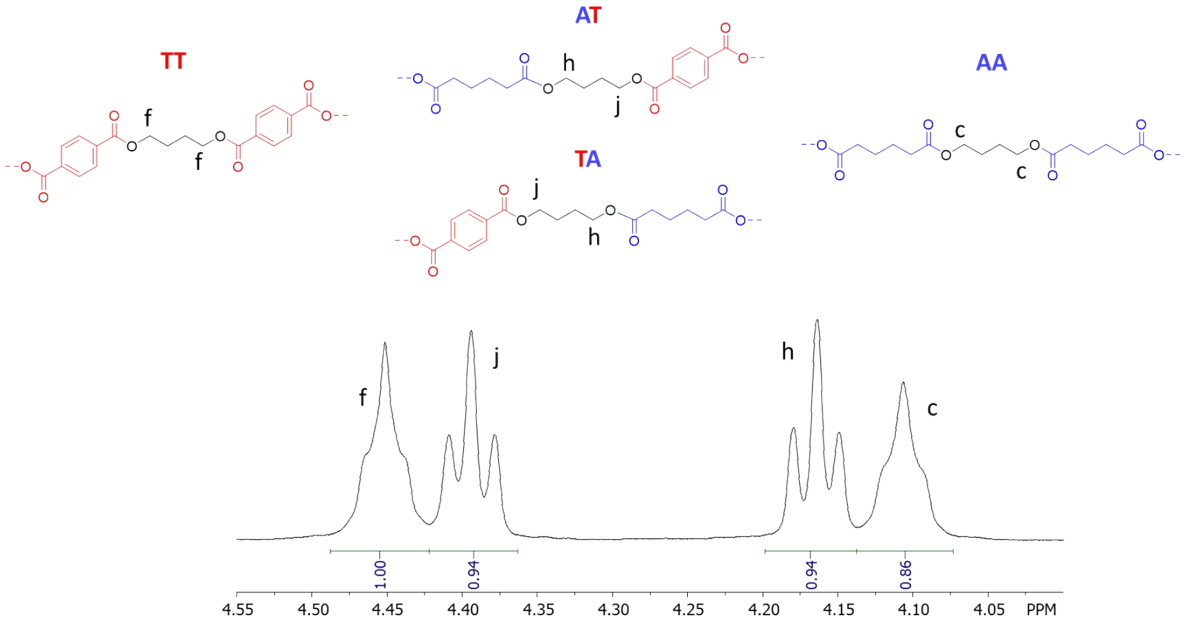

Figure S14. Zoomed-in figure of the ^{1}H-NMR spectrum of vPBAT in $CDCl_3$ for sequence distribution calculations.

The molar fraction of each dyad was calculated from the ^{1}H NMR spectrum using the area of the signals corresponding to the TT, AT, TA, and AA units according to Eq. 1-4. The probability factors, the sequence length, and the degree of randomness were calculated using Eq. 5-6, Eq. 7-8, and Eq. 9 respectively.

Eq. 1

$$f_{AA} = \frac{A_c}{A_h + A_j + A_c + A_f}$$

Eq. 2 $$f_{AT} = \frac{A_h}{A_h + A_j + A_c + A_f}$$

Eq. 3 $$f_{TA} = \frac{A_h}{A_h + A_j + A_c + A_f}$$

Eq. 4 $$f_{TT} = \frac{A_f}{A_h + A_j + A_c + A_f}$$

Eq. 5 $$P_{AT} = \frac{f_{AT}}{f_A}$$

Eq. 6 $$P_{TA} = \frac{f_{TA}}{f_T}$$

Eq. 7 $$L_{nA} = \frac{1}{P_{AT}}$$

Eq. 8 $$L_{nT} = \frac{1}{P_{TA}}$$

Eq. 9 $$r = P_{AT} + P_{TA}$$

f_{XX} is the molar fractions of the AA, AT, TA, and TT segments respectively. A_X is the area of the integral for the protons (f, j, h, and c) corresponding to the AA, AT, TA, and TT segments respectively. P_{AT} is the probability of encountering a terephthalate unit next to an aliphatic segment. f_A is the molar content of adipate units in the polymer. f_T is the molar content of terephthalate units in the polymer. L_{nA} = average sequence length of the aliphatic segment. L_{nT} = average sequence length of the aromatic segment. r = Degree of randomness.

Table S2. Sequence distribution of the PBAT samples.

Polymer	f_{TT}	f_{TA}	f_{AT}	f_{AA}	f_A	f_T	P_{TA}	P_{AT}	L_{nA}	L_{nT}	r
cPBAT	0.23	0.26	0.25	0.26	0.52	0.49	0.53	0.49	2.04	1.90	1.02
rPBAT	0.27	0.25	0.25	0.23	0.49	0.51	0.50	0.52	1.94	2.02	1.01
vPBAT	0.27	0.25	0.25	0.23	0.49	0.52	0.49	0.52	1.93	2.05	1.01

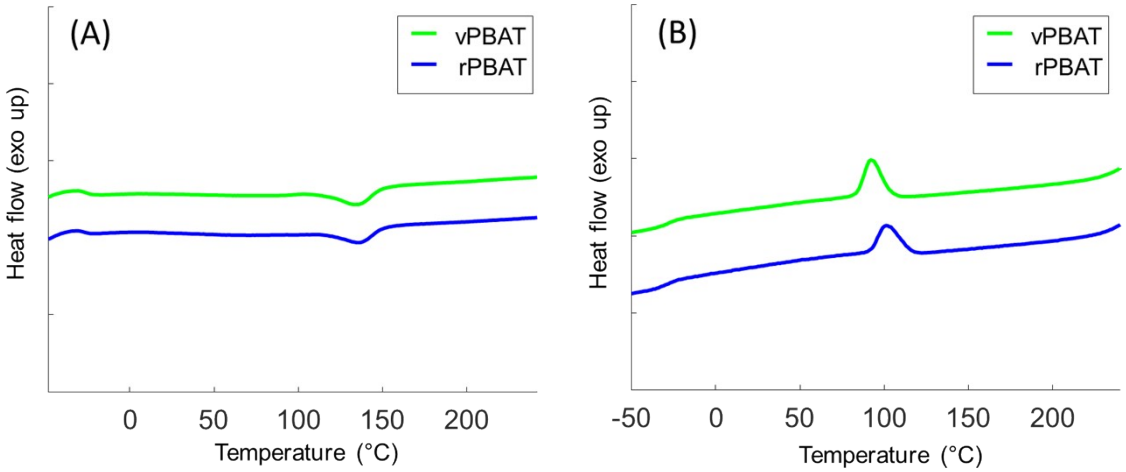

Figure S15. (A) DSC second heating, and **(B)** first cooling curves of the synthesized PBAT using commercial monomers (vPBAT) or recycled monomers (rPBAT).

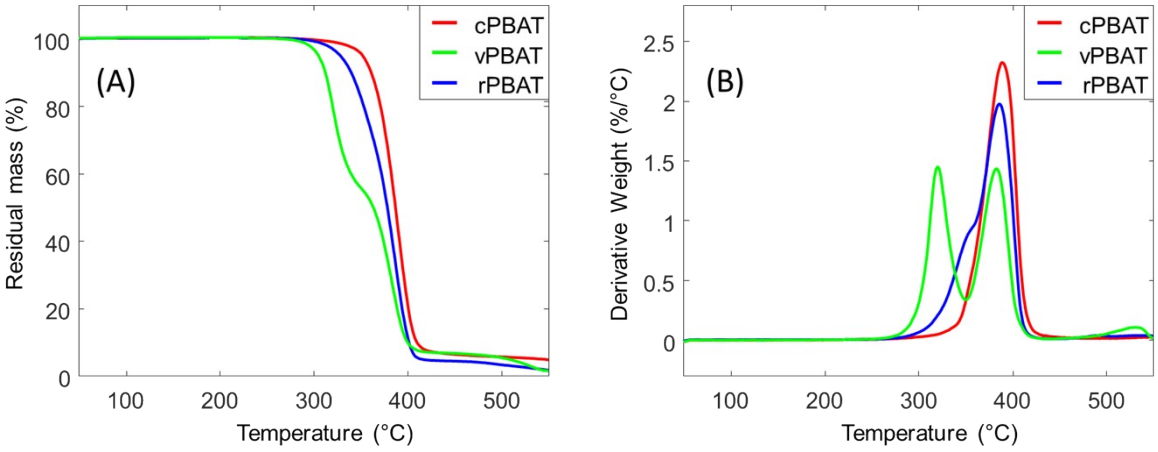

Figure S16. (A) TGA weight loss, and **(B)** first derivative weight loss thermograms of the commercial PBAT (cPBAT), and synthesized PBAT using commercial monomers (vPBAT) and recycled monomers (rPBAT), respectively.

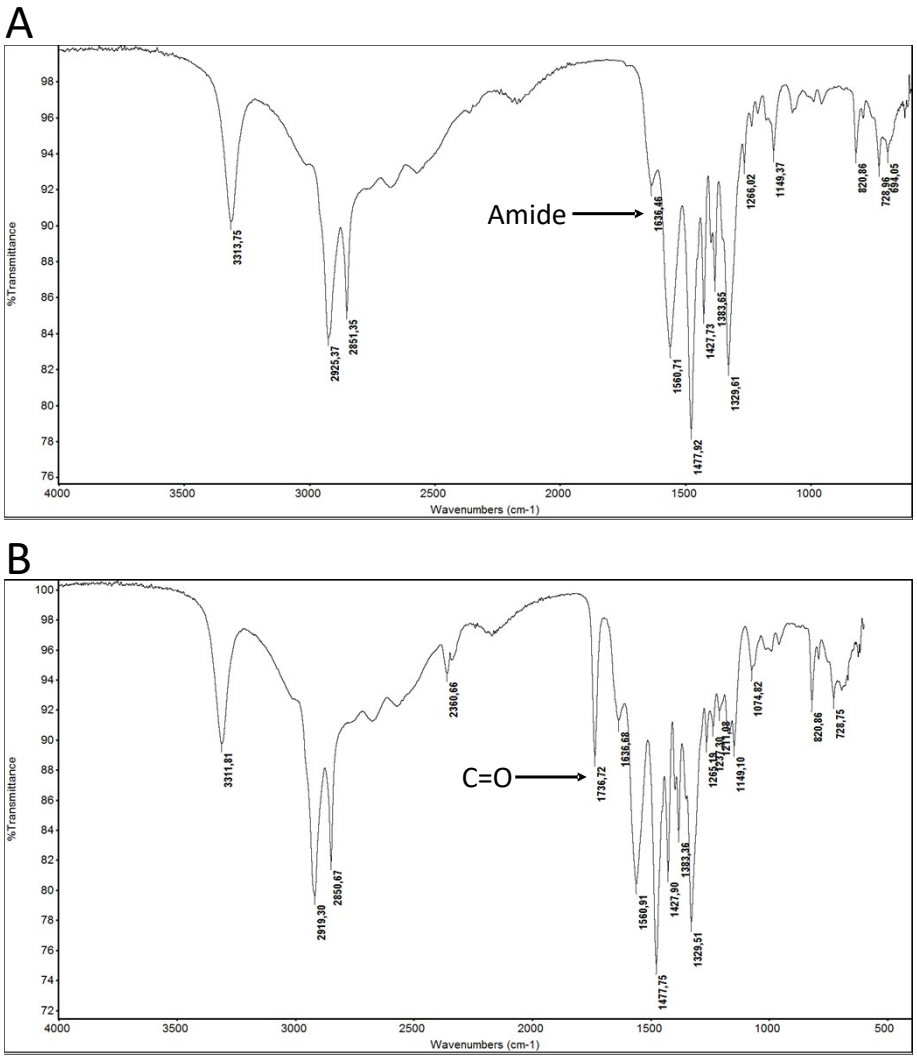

Figure S17. FTIR analysis of the polymerization reaction between adipic acid and hexamethylenediamine in toluene: (A) catalysed by 10 % (w/w) Novozym®435, and **(B)** without the biocatalyst.

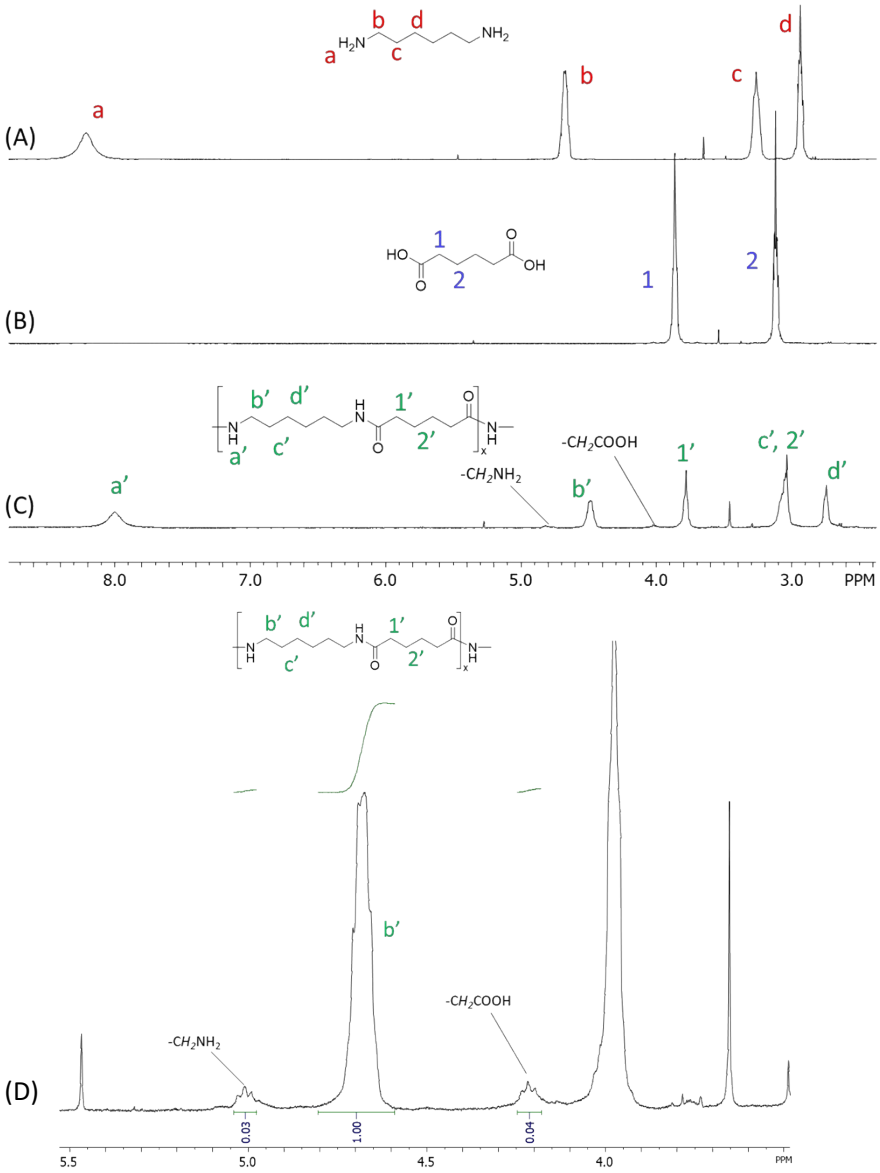

Figure S18. ^{1}H-NMR spectra of hexamethylenediamine **(A)**, adipic acid **(B)**, and crude Nylon 6,6 **(C)** in TFA-*d*. M_n of 3500 g mol^{-1}; 47 % HMDA and 53 % AA incorporated in the polyamide. In a previous study, the synthesis of Nylon 8,10 using Novozym®435 resulted in a polymer with M_n of 520 g mol^{-1}; the molecular weight was however improved by increasing the CalB load, increasing the temperature, and applying vacuum in a multistep reaction resulting in M_n of 4960 g mol^{-1}.[2] The longer alkyl chain diamines are preferred as they increase the chances for the enzyme to access the bonds, and hence higher molecular weight can be obtained (as in Nylon 8,10 compared to Nylon 6,6). **(D)** Zoomed in ^{1}H-NMR spectrum in TFA-d of the end groups of the crude Nylon 6,6.

The number average molecular weight of the crude Nylon 6,6 was calculated accordingly:

M_{HMDA} = 116.21 g mol^{-1}

M_{AA} = 146.14 g mol^{-1}

$M_{Repeating\ Unit}$ = (116.21 + 146.14) - 36 = <u>226.35</u> g mol^{-1}

$A_{end\ groups}$ = 0.03 + 0.04 = 0.07

$A_{\text{Repeating Unit}} = 1$

$n_{\text{end groups}} = A_{\text{Repeating Unit}} / A_{\text{end group}} = \underline{14.3}$

$M_n = 226.35 \text{ g mol}^{-1} * 14.3 + 116.21 \text{ g mol}^{-1} + 146.14 \text{ g mol}^{-1} = \underline{3466} \text{ g mol}^{-1}$

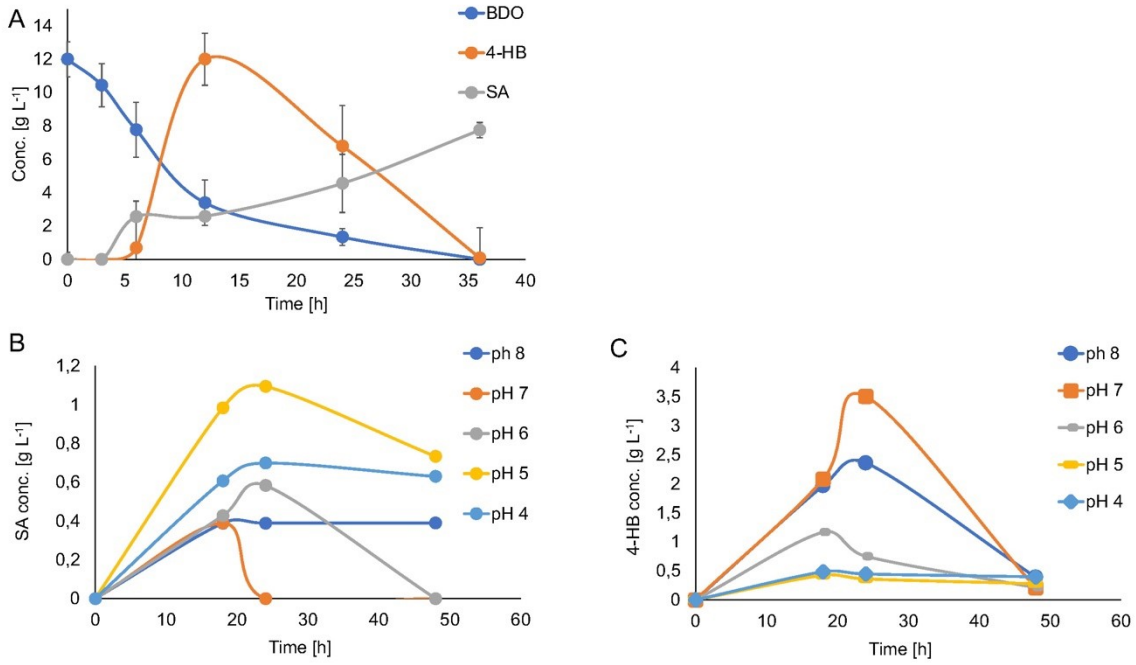

Figure S19. Consumption of 1,4-butanediol (BDO) and formation of 4-hydroxybutyrate (4-HB) and succinic acid (SA) during oxidation of 10 g L^{-1} (130 mM) BDO by *G. oxydans* resting cells. **(A)** Starting pH was set to 7 without pH control during the reaction time. **(B)** SA formation and **(C)** Effect of pH on 4-HB formation from 1 g L^{-1} BDO using *G. oxydans* resting cells (OD_{600} = 10) in reactions initially set at different pH values without further pH control throughout the reaction time. The reactions were performed in duplicates and the plots represent the mean of the measurements.

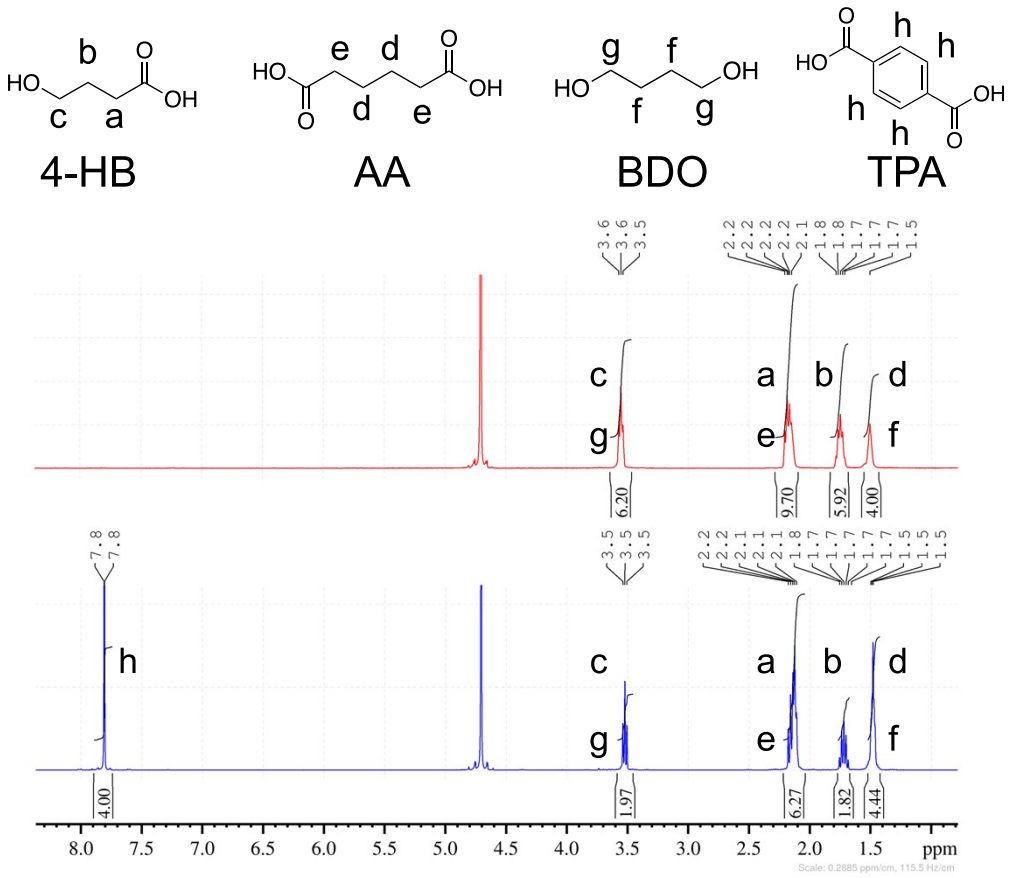

Figure S20. ^{1}H-NMR analysis in D_2O for the oxidation of BDO present in nanofiltration (red) and ultrafiltration (blue) permeate fractions using *G. oxydans*. 4-HB signals are assigned, the rest are for AA and BDO, and TPA in case of UF-permeate fraction.

Table S3. Comparison of enzymatic degradation of PBAT described in literature and this study.

Enzyme	Expression conditions	Substrate	Reaction conditions	Degradation products	References
PpEst Esterase (*Pseudomonas pseudoalcaligenes*)	*E. coli* BL21-Gold(DE3) for 20 h at 25°C	PBAT film	10 mg of milled PBAT or 100 mm^2 of PBAT film in 100 mM potassium phosphate buffer pH 7.0 were mixed with 5 µM of PpEst enzyme at 50-80 °C	At 65°C the activity was 7 times higher on the milled PBAT film than on the whole film.	3
PfL1 lipase (*Pelosinus fermentans* DSM 17108)	*E. coli* BL21 Gold(DE3) for 20 h at 20°C	PBAT film as well as milled PBAT	5x10 mm PBAT film as well as 10 mg milled PBAT were incubated with 0.6 µM of PfL1 in 0.1 M sodium phosphate buffer pH 7.5 at 50 °C, 100 rpm for 72h	Higher degradation rates were observed with the milled PBAT. The order of the depolymerization products was as follows: BDO-TPA[a]>BDO-TPA-BDO[b]>TPA	4
PCLE cutinase (*Paraphoma*-related fungal strain B47-9)	Produced in *Paraphoma sp.* B47-9 strain and purified from the culture medium	PBAT Ecoflex F Blend C1200	Film was incubated with 50 µL of PCLE (10 µg mL^{-1} in 25 mM HEPES-NaOH buffer pH 7.2 containing 1 mM $CaCl_2$) at 30 °C for 24 h	Degradation was confirmed via measuring the water-soluble total organic carbon (TOC)	5
Tcca carboxylesterase (*Thermobacillus composti* KWC4)	*E. coli* BL21(DE3) 16 °C for 20 h	PBAT film	8 mm × 8 mm PBAT film incubated with 10.9 µM enzyme in 0.8 mL 100 mM PBS buffer pH 8.0, 300 rpm at 40 °C for 48h	After 24h, 4 µM TPA per mole protein was detected	6

Ple628 and ple629 PETase-like hydrolase (from marine microbial consortium)	*E. coli Origami* (DE3), TB medium, 16°C for 20 h	Ecovio®FT 2341	0.156 µM of Ple628 or Ple629 were incubated with 5 mg of Ecovio®FT film in PBS at 30°C for 72h	Ple629 showed higher activity compared to Ple628 releasing 1103.6 µM of BDO-TPA[a] after 72h	7
Cbotu_EstA and Cbotu_EstB esterases *(Clostridium botulinum* ATCC 3502)	*E. coli* BL21 Gold(DE3) 20°C for 20 h	Oligomeric PBAT model substrates and PBAT film	0.6 µM enzymes incubated with 10 mg PBAT for 72 h in 50 mM potassium phosphate pH 7.0 at 50 °C for Cbotu_EstA and 37 °C for Cbotu_EstB	Only Cbotu_EstB showed marginal activity on PBAT. Both enzymes were active against low molecular weight model substrates BDO-TPA-BDO[c] and BDO-TPA-BDO-TPA-BDO[d]	8
***TcCut* cutinase (*Thermobifida cellulosilytica*)**	*E. coli* BL21(DE3) 16 °C for 20 h	PBAT film	10 µg mL^{-1} enzyme incubated with PBAT film (1 ×1 cm) in 50 mM glycine-NaOH buffer (pH 9.0) at 65 °C, 800 rpm for 48h	5198 mol of TPA and BDO-TPA_a per mol enzyme	9
TfCut* cutinase *(Thermobifida fusca)	*E. coli* BL21(DE3) 16 °C for 20 h	PBAT film	10 µg mL^{-1} enzyme incubated with PBAT film (1 ×1 cm) in 50 mM glycine-NaOH buffer (pH 9.0) at 70 °C, 800 rpm for 48h	5361 mol of TPA and BDO-TPA[a] per mol enzyme	9
LCC-WCCG cutinase (uncultured bacteria)	*E. coli* BL21(DE3) 16 °C for 20 h	PBAT film	1 µM enzyme incubated with PBAT (25 g L^{-1}) in 100 mM potassium phosphate buffer pH 8, 75 °C.	226 027 mol of TPA, AA, and BDO per mol LCC-WCCG = 3390 mol TPA per mol LCC-WCCG 129 966 mol BDO per mol LCC-WCCG 93 670 mol AA per mol LCC-WCCG	This study

[a,b,c,d] Oligomers formed from respective monomer units

References

1 V. Tournier, C. M. Topham, A. Gilles, B. David, C. Folgoas, E. Moya-Leclair, E. Kamionka, M. L. Desrousseaux, H. Texier, S. Gavalda, M. Cot, E. Guémard, M. Dalibey, J. Nomme, G. Cioci, S. Barbe, M. Chateau, I. André, S. Duquesne and A. Marty, *Nature*, 2020, **580**, 216–219.

2 L. Ragupathy, U. Ziener, R. Dyllick-Brenzinger, B. Von Vacano and K. Landfester, *J. Mol. Catal. B Enzym.*, 2012, **76**, 94–105.

3 P. W. Wallace, K. Haernvall, D. Ribitsch, S. Zitzenbacher, M. Schittmayer, G. Steinkellner, K. Gruber, G. M. Guebitz and R. Birner-Gruenberger, *Appl. Microbiol. Biotechnol.*, 2017, **101**, 2291–2303.

4 A. Biundo, A. Hromic, T. Pavkov-Keller, K. Gruber, F. Quartinello, K. Haernvall, V. Perz, M. S. Arrell, M. Zinn, D. Ribitsch and G. M. Guebitz, *Appl. Microbiol. Biotechnol.*, 2016, **100**, 1753–1764.

5 K. Suzuki, M. T. Noguchi, Y. Shinozaki, M. Koitabashi, Y. Sameshima-Yamashita, S. Yoshida, T. Fujii and H. K. Kitamoto, *Appl. Microbiol. Biotechnol.*, 2014, **98**, 4457–4465.

6 P. Wu, Z. Li, J. Gao, Y. Zhao, H. Wang, H. Qin, Q. Gu, R. Wei, W. Liu and X. Han, *Catalysts*, 2023, **13**, 340.

7 I. E. Meyer Cifuentes, P. Wu, Y. Zhao, W. Liu, M. Neumann-Schaal, L. Pfaff, J. Barys, Z. Li, J. Gao, X. Han, U. T. Bornscheuer, R. Wei and B. Öztürk, *Front. Bioeng. Biotechnol.*, 2022, **10**, 930140.

8 V. Perz, A. Baumschlager, K. Bleymaier, S. Zitzenbacher, A. Hromic, G. Steinkellner, A. Pairitsch, A. Łyskowski, K. Gruber, C. Sinkel, U. Küper, D. Ribitsch and G. M. Guebitz, *Biotechnol. Bioeng.*, 2016, **113**, 1024–1034.

9 Y. Yang, J. Min, T. Xue, P. Jiang, X. Liu, R. Peng, J. W. Huang, Y. Qu, X. Li, N. Ma, F. C. Tsai, L. Dai, Q. Zhang, Y. Liu, C. C. Chen and R. T. Guo, *Nat. Commun.*, 2023, **14**, 1645.